VII International Conference on Computational Methods for Coupled Problems in Science and Engineering
COUPLED PROBLEMS 2017
M. Papadrakakis, E. Oñate and B. Schrefler (Eds)

TRANSPOSITION OF A WEIGHTED AH-THROUGHPUT MODEL TO ANOTHER LI-ION TECHNOLOGY: IS THE MODEL STILL VALID? NEW INSIGHTS ON THE MECHANISMS

T. DELETANG [*] N. BARNEL [*] S. FRANGER[†] L. ASSAUD[†]

[*] EDF - R&D – Lab Les Renardières
Département LME / Groupe M2A
Avenue des Renardières - Ecuelles
77818 MORET SUR LOING Cedex FRANCE
e-mail: tiphaine.deletang@edf.fr

[†] Université Paris-Sud – Orsay
Institut de Chimie Moléculaire et des Matériaux d'Orsay
Bâtiment 410/420/430, Université Paris-Sud 11
Rue du Doyen Georges Poitou
91400 ORSAY – FRANCE

Key words: Storage, Lithium-ion cells, Fatigue model, Eyring and Arrhenius kinetics, Butler-Volmer

Abstract: The increasing interest in electric vehicles powered by rechargeable batteries, combined with the wide development of powerful lithium-ion batteries as a renewable energy storage system have raised the need for battery ageing characterization. Several models have been developed for this purpose, including empirical, fatigue and mathematical ones. One of the main issue of these approaches consists of the universality, when extension is required to other chemistries or solicitations. Electrochemical models are supposedly the most extensible. The Weighted Ah-Throughput Model takes into account that certain operating conditions may lead either to an increase or a decrease of the rate of ageing. It modulates the impact of the exchanged Ah by the temperature, the C-rate and the state of charge (SOC), both in calendar and active regime. This influence of the parameters is described here, and compared between two Li-ion chemistries: LFP and NCA. The similitudes enable us to extract the generic hidden mechanisms that, by nature, the fatigue modelling methods do not provide. This innovative method enables us to reach energetic behavior laws. We finally suggest improvements on the tests matrix used to define the model, to better fit the outcome of the study.

1 INTRODUCTION

For lithium-cells to be used in electric vehicles or stationary storage, they have to perform over a long period. However, lithium-cells performances decrease over time, both when they are used (on cycling) and when they are on storage. The ageing is caused mainly by a primary mechanism of a passive layer growing at the negative electrode, corresponding to the so-called solid-electrolyte interphase (SEI), therefore causing the loss of lithium ions cyclability, finally decreasing the total capacity. [1,2,3] This phenomena is mainly responsible for the ageing during active and inactive regimes (pure storage). Another cause of ageing is due to the presence of mechanical defaults in the bulk material at the positive electrode, caused by repeated insertion and deinsertion of lithium ions inside the structure. [4] The lithiation process taking place mainly during the cycling of the battery, it will be neglected during temporal regime. [1]

Current models tend to base the ageing rate of the cell on the solicitation of the batteries. Our approach is different. We consider the ageing to be due to three main parameters, which are temperature, state of charge and rated-current. In this paper, an existing fatigue model for the capacity loss [1] is explored, and is used to analyse our ageing data coming from our cells. Weighting functions distinguishing the impact of temperature, SOC and rated-current are drawn for them. They are compared with the ones already obtained for cells with another chemistry [1]. The two curves will be studied in order to exhibit and discuss the associated mechanisms.

2 EXPERIMENTAL

A 2.4Ah commercial lithium-ion cell based on graphite/iron-phosphate (LiFePO4) called LFP is aged. The battery basic characteristics can be seen in Table 1. The characterization tests were performed using Bitrode platform.

Table 1: LFP cell basic characteristics

Cell	Capacity	Cut-off voltages	Charging Protocol
LFP	2.4Ah	3.65V / 2.45V	CC-CV

The cells were initially virgin before performing the tests. A total of 11 different ageing tests were performed, including 3 different temperatures, 5 different SOC (10%, 50%, 80%, 95%, 100%) and 2 rated-currents. They are either cycled (9 cells) or stored (2 cells). The tests are detailed in the Table 2.

Table 2: Tests matrix

	T (°)	SOC (%)	$I_c(A.Ah^{-1})$	$I_d\ (A.Ah^{-1})$
1	T1	80		
2	T2	80		
3	T1	10	1C	1D
4	T1	50	1C	1D
5	T1	80	1C	1D
6	T1	95	1C	1D
7	T1	100	1C	1D
8	T1	100	C/2	1D
9	T1	100	1C	D/2
10	T2	100	1C	1D
11	T3	100	1C	1D

For each ageing condition, one cell only was used. The cell charging protocol consists on a constant current charge followed by a constant voltage phase (CC-CV). Regularly, every two weeks in average, performance check-ups were performed. The protocol consists in a full CC-CV charge, followed by 30 minutes of rest. Then the capacity is measured counting the discharged ampere-hours at 1D and at the same temperature as the test.

3 MODEL

The rate of each ageing mechanism for a specified chemistry cell is considered in the model to be a function of the mode of operation: cycling or storage. It results in two types of degradation: active degradation, and calendar degradation, the latter appearing both during cycling and storage. The work of Badey [1] integrates this ageing inside an original fatigue model. First, it demonstrates that the irreversible loss of capacity can be calculated by summing these two degradation contributions. Then, according to the author, the decoupling of the two degradations (active and calendar) is ensured by the Weighted Ah-Throughput Model (WTM) which is a modified approach of the Ah-throughput counting method. Both methods consider the ageing as a function of the Ah exchanged and the time. The originality lays in the fact that when the Ah-counting method takes into account only these parameters (Ah exchanged and time), the WTM integrates additionally the strong impact of the operating conditions on the rate of ageing. Therefore it modulates the impact of both modes of degradations by the temperature, the C-rate and the state of charge (SOC), as written in Equation 1.

$$\Delta Q = f(T, I, SOC).Ah + g(T, I, SOC).\sqrt{t} \quad (1)$$

$$\Delta Q = K^{cyc} f_1(T) f_2(I) f_3(SOC).Ah + K^{cal} g_1(T) g_2(I) g_3(SOC).\sqrt{t} \quad (2)$$

(1) The rate is abusively written as I.

Due to the growth of the SEI layer, the calendar life capacity fade typically follows a $\sqrt{t}$-kinetic law. [5] The $f_i(X)$ (resp. $g_i(X)$) function corresponds to the active regime (resp. calendar) ageing contribution attributable to X (T, I or SOC). They are multiplied that way because we consider all the parameters to be intertwined. They have been chosen as dimension-less functions. K^{cyc} and K^{cal} holds the dimensions [%Ah/Ah] and [%Ah.$s^{-0.5}$] respectively.

4 RESULTS

The tests matrix, conceived in order to vary the parameters (T, I or SOC) one by one in each test, is applied on cells based on graphite/iron-phosphate (LiFePO4, LFP. From the cycles' results, we compute the Ah exchanged, and from the check-ups results, we compute the corresponding loss of capacity. Equation 1 can be rewritten as:

$$\frac{\Delta Q}{\sqrt{t}} = K^{cyc} f_1(T) f_2(I) f_3(SOC).\frac{Ah}{\sqrt{t}} + K^{cal} g_1(T) g_2(I) g_3(SOC) \quad (3)$$

A linear regression leads to two proportion coefficients: the multiplicative product of f_i and the multiplicative product of g_i. The first step is to split it apart to determine each element $f_i$and g_i separately. The method used is described in [1]. We can then compute and interpolate the data points obtained for each f_i and g_i.

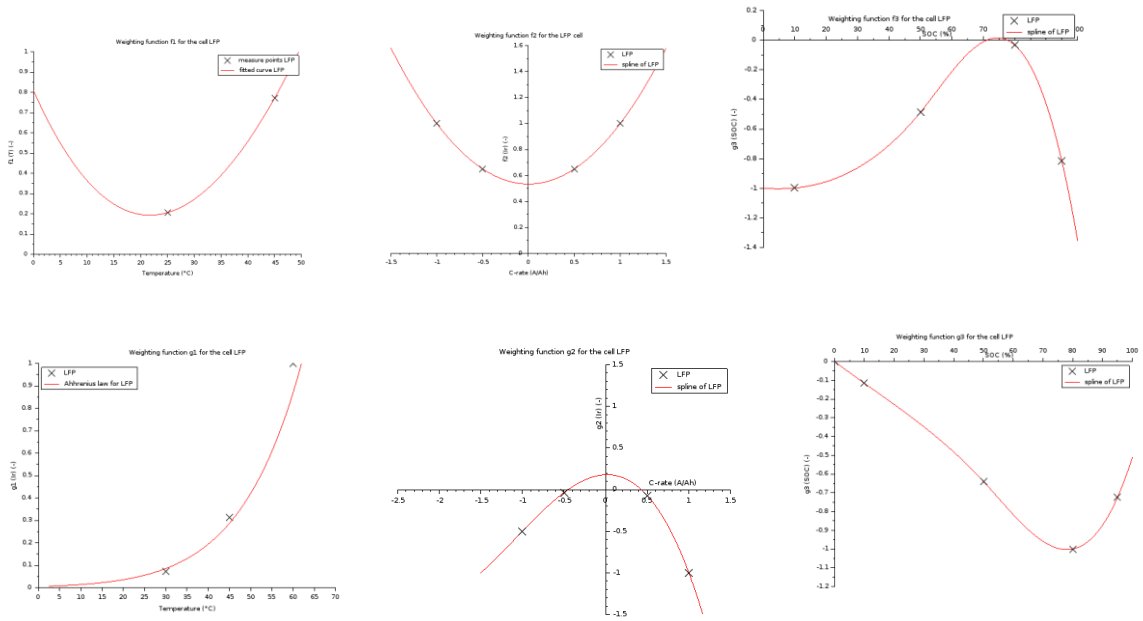

Figure 1: Weighting functions obtained for LFP, obtained for both calendar and cycles ageing. From top to bottom, left to right: f1(T), f2(I), f3(SOC), g1(T), g2(I), g3(SOC).

It has to be noticed that these functions are assumed to be dependent on the Li-ion composition, chemistry, manufacturing, casing, etc. [6,7] Therefore, they have to be computed again for other types of cells models.

Nevertheless, this paper studies the similarities between these functions. Functions coming from the LFP/graphite cells have been compared with the ones coming from literature regarding $LiNi_{0.8}Co_{0.15}Al_{0.05}O_2$/graphite (NCA) cells.

5 DISCUSSION

5.1 Discussion on the g_3 curve

The function g_3 has been chosen negative. Figure 2 shows that the two curves are very similar: a minimum range of values is observed both on NCA and LFP. It corresponds to a maximum impact of the SOC on the calendar ageing. This means that the passivation layer speed is maximum around that average SOC.

Repeating the same modelling, but considering the exchanged watt-hours (and no more the exchanged ampere-hours), we compute the same kind of linear regression:

$$\Delta Q = f^{Wh}(T,I,SOC).Wh + g^{Wh}(T,I,SOC).\sqrt{t} \quad (4)$$

By writing it in an infinitesimal way, we have:

$$\Delta Q = f^{Wh}(T,I,SOC).\delta E + g^{Wh}(T,I,SOC).\sqrt{\delta t} \quad (5)$$

As seen previously (Equation 1), we have:

$$\Delta Q = f^{Ah}(T,I,SOC).dq + g^{Ah}(T,I,SOC).\sqrt{\delta t} \quad (6)$$

On the interval $[50\%;80\%]$ the numerical values show that $g^{Ah}(T,I,50\%) = g^{Wh}(T,I,50\%)$ and therefore, Equation 5 gives $f^{Ah}(T,I,SOC).dq = f^{Wh}(T,I,SOC).\delta E$. We were expecting only one value of extreme SOC, we end up having a range of values.

We can conclude that on this interval, $\delta E = \frac{f^{Ah}(T,I,SOCmin)}{f^{Wh}(T,I,SOCmin)}.dq$, the lost energy during cycling derives from a potential. We find here a behaviour law, independent from the SOC, the latter being not a thermodynamic variable. On this range of SOC, we are independent from the chemistry, this electrical potential accounts for the entire behaviour. This totally confirms our plan to work towards an equivalent circuit model.

Concerning the trial, it shows that it is enough to focus on one SOC (chosen at 50%) to account for the behaviour of the cell at the neighbourhood of 50%.

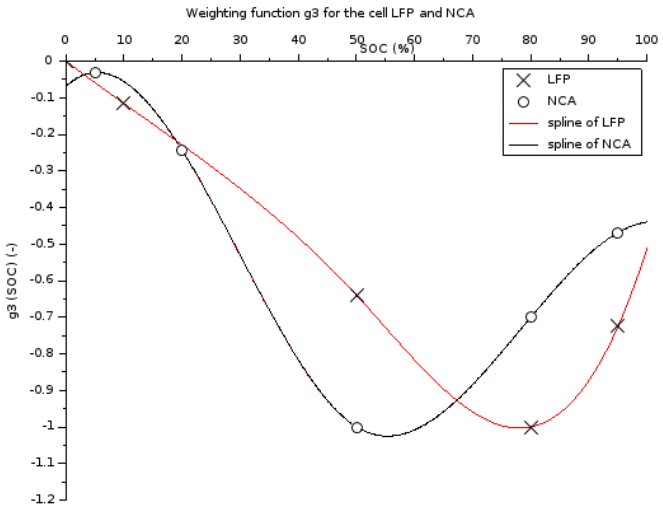

Figure 2: Weighting function g3 for NCA and LFP. Markers represent experimental values.

5.2 Discussion on the f_1 and the g_1 curve

The g_1 function represents the influence of the temperature on the ageing occurring during pure storage.

The g_1 curve, associated with the g_1 function, can be fitted by an Arrhenius law, which represents the speed of the electrochemical reaction depending on the temperature: $g_1(T) = \lambda.e^{\frac{-E_A}{RT}}$. This is coherent with the fact that the calendar ageing is due to the electrolyte

decomposition, and the subsequent SEI formation. [8] The NCA curve has been fitted from experimental values. The difference between both chemistries laws lays in the activation energy value. (Figure 3)

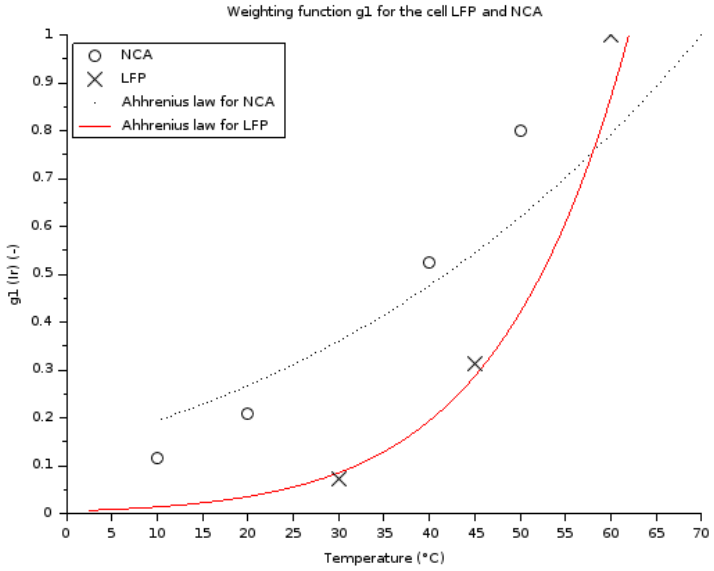

Figure 3: Weighting function g1 for NCA and LFP. Markers represent experimental values.

The f_1 function represents the influence of the temperature on the ageing occurring while battery is cycled. The f_1 curve interpolates the experimental values.

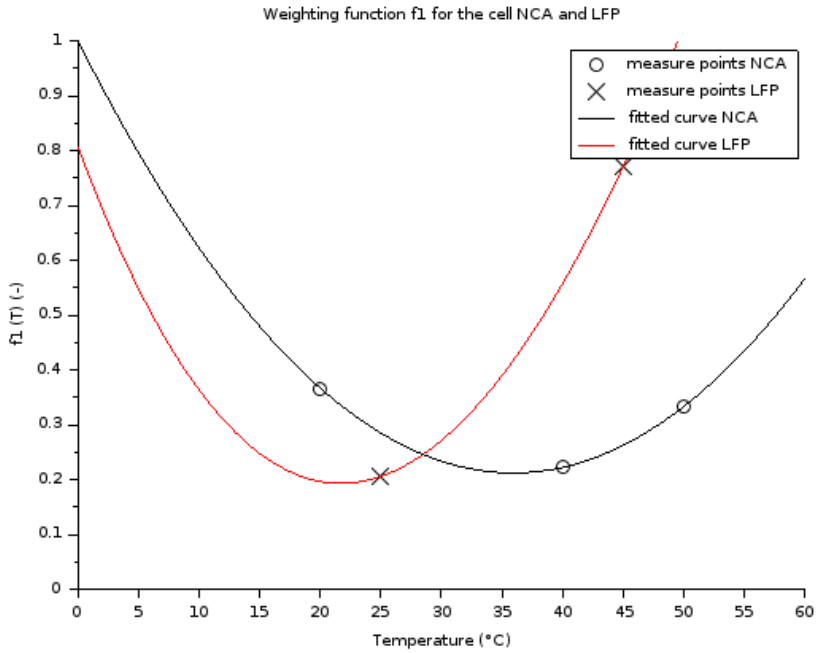

Figure 4: Weighting function f1 for NCA and LFP. Markers represent experimental values.

Again, we can see on Figure 4 that the two curves have the same shape, and shows an extremum of ageing around the same temperature.

Molecular-level understanding of solid-electrolyte interphase (SEI) growth kinetics has been considered as part of a transition state theory, which accounts for the effect of the temperature on the growth rate. This relationship is called the Eyring's law, and is quite similar to the Arrhenius law. We use the so-called Eyring law to point out the speed of the side reaction taking place in the battery cell.

$$k(T) = \alpha.\frac{k_B T}{h}.e^{\frac{-\Delta G_0}{RT}} \tag{7}$$

Where k is the speed constant, related to the degradation rate, h is the Planck constant, R is the gas constant (J.K−1.mol−1). According to the literature, there are reviews providing with some similar models [9]. However these models do not distinguish the SOC from the temperature, simply suggesting a 3D fitting with both parameters taken into account.

The current is linked to the speed constant by the Butler-Volmer law: $i(T) = \lambda.k(T).\left(e^{\frac{-A}{T}} - e^{\frac{B}{T}}\right)$, where λ, A and B are constants.

On the other hand, John Newman explains that the cells generate their own heat. He shows that the energy balance is made of two terms. The first one is associated with the Joules effect, considered as irreversible, and the second one is due to the heat generation at the interface between the electrolyte and the electrode, therefore it is reversible. The irreversible heating source has been described by Hemery [10]:

$$\frac{\partial Q_{irr}}{\partial t} = i(T).[(U - U_{ocv}) + T * \frac{\partial U_{ocv}}{\partial T}] \tag{8}$$

At the first order, $\frac{\partial U_{ocv}}{\partial T}$ is considered to be constant and $U - U_{ocv} = R.i$.
Therefore, Equation (8) becomes:

$$Q_{irr} = i.[R.i + T.\gamma].dt \tag{9}$$

$$Q_{irr} = [R.i + T.\gamma].Ah \tag{10}$$

So, by definition, $f_1(T)$ is proportional to $R.i + T.\gamma$, so, $\frac{f_1(T)}{T} = \mu.\frac{i(T)}{T} + \theta = \varepsilon\left(e^{\frac{-A}{T}} - e^{\frac{B}{T}}\right) + \xi$.
The constant ε has been arbitrarily set equal to 1. From the three points coming from NCA tests, a relationship between A and B can be found: $B = 1.02.A$..Therefore two unknowns are remaining (A and ξ), which is enough to fit the two measurement points obtained for LFP. The fit for NCA and LFP can be seen on Figure 4.

This minimal temperature is thermodynamically justified, the others appear as deviations from ideality.

5.3 Discussion on the f_2 and the g_2 curve

The f_2 function represents the impact of the rated-current on the ageing appearing while cycling.

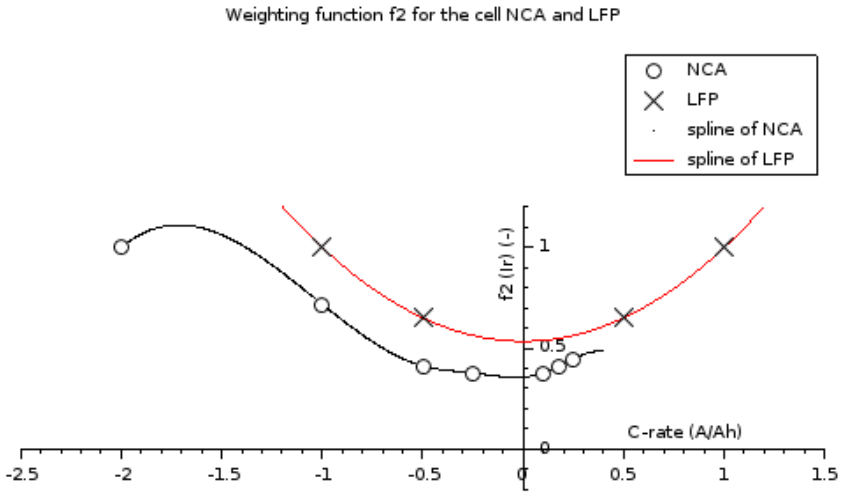

Figure 5: Weighting function f2 for NCA and LFP. Markers represent experimental values.

The LFP curve and the NCA have been fitted with a spline, resulting in polynomial functions. We can see the two curves have a similar shape and are odd around zero.

The g_2 function represents the impact of the rated-current on the ageing appearing during calendar ageing (both in cycling and pure storage).(Figure 6)

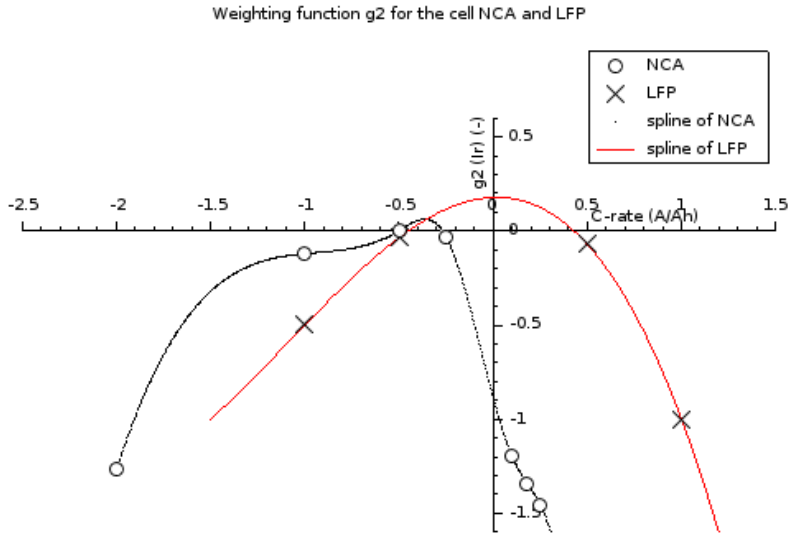

Figure 6: Weighting function g2 for NCA and LFP . Markers represent experimental values. The spline interpolates the data coming from LFP, when the charge and discharge temperature has not been distinguished

The LFP and the NCA curves have been fitted with a spline (Figure 6). However, for the NCA cells, the tests did not feature a constant temperature, due to heating of the internal resistance. Therefore, the charge temperature and the discharge temperature impact had to be differentiated. First both temperatures had to be reconstituted. The method used is detailed in

[1]. This difference is due to a depth of discharge of 100% applied to the cells. However, for the LFP cells, the difference between both temperatures is too small for the method to be relevant.

There seem to exist a relation between the impact of C-rate in charge and the impact in discharge.

Mechanical deformations of the active material are assumed to be responsible for ageing in cycling [11]. Therefore, the f_2 function should explain this phenomena.

We have to keep in mind that lithium-ion cells convert chemical energy to electric energy via redox reaction originating from both lithium-ion motion and electron transfer under a certain applied potential. The ions have the lowest energy when they are intercalated inside the positive electrode (cathode) and highest energy when they are in the negative electrode (anode). Considering cations, this corresponds to low (resp. high) potential accordingly. This electrochemical reaction allows the lithium ions to transfer from the solid phase (the electrode) towards the solution (the electrolyte), via intercalation currents, and vice versa. [12]

The reaction corresponds to the intercalation / deintercalation of lithium ions in the graphitic layers at the anode and in the active material (LFP or NCA) structure at the cathode. [12] The charge transfer is considered to be the limiting factor since the mass transport is insured by a highly ionic concentrated electrolyte. The charge transfer speed decreases with time due to the decay of conductivity in the electrolyte [7] and decrease of the active surface at the electrode.

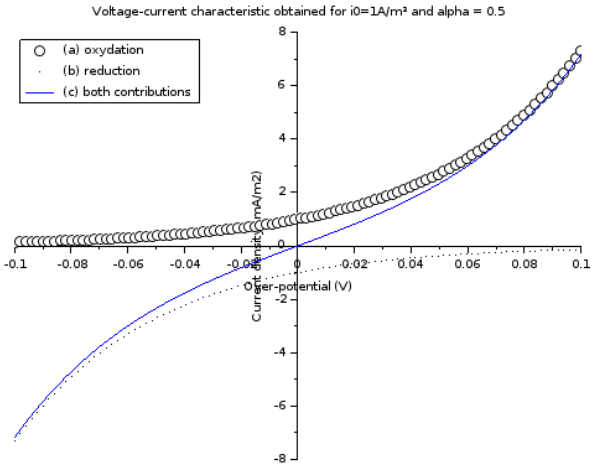

Figure 7 Voltage-current characteristic. (a) oxydation (b) reduction (c) total of both contributions. Markers represent experimental values.

The current-voltage characteristic of this electrode is given by its Butler-Volmer relationship: $i = i_0(e^{\frac{\alpha nF\eta}{RT}} - e^{\frac{-(1-\alpha)nF\eta}{RT}})$, which makes it an odd curve (see Figure 7), where i is the current (A) at the electrode, T the temperature (K), R the molar gas constant (R=8.1345J/(mol.K)), F the Faraday constant (F = 96 485,3329 sC/mol-1), η is the over-potential ($\eta = E - E_{eq}$) and E the electrode potential, i_0 is related to the charge transfer speed constant and the concentration of the Li^+ (in the electrolyte and in the electrode), α

characterizes the symmetrical aspect of the charge transfer. We assume that one electron is involved in the reaction (n=1).

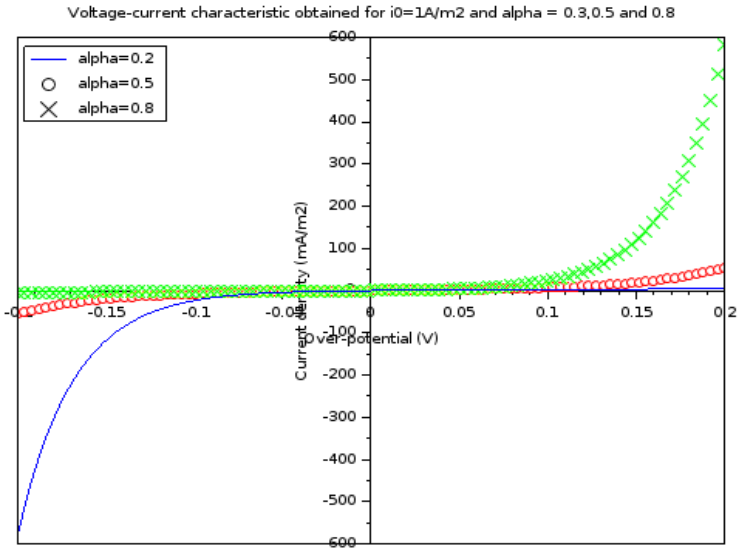

Figure 8 Voltage-current characteristic for different values of alpha coefficient. Markers represent experimental values.

The coefficient of interest is α : when α is close to 0, the over-potential η essentially leads to the reduction of the electrolyte, whereas when it is close to 1, it essentially induces its oxydation. When it is equal to ½ , it means that the over-potential equally affects the activation barrier of oxidation and reduction.(see Figure 8). It accounts for the passive film SEI growth, and whether it is formed rather in charge or in discharge. This provides information on the ability of the insertion and deinsertion of Li^+in the graphitic layers at the anode. The two reactions (growth of the SEI and intercalation of lithium-ion) are correlated. It chemically represents the distance between the activated complex and the final product. For high values of α, the reaction is supposedly easily activated, as the final product is close to the intermediate one.

Approximating the Butler-Volmer equation around the high over-potential regions, ($|\eta| \gg \frac{RT}{F}$ and $\eta > 0$) a limited development of e^x= 1+x of the intensity gives $i = i_0\left(e^{\frac{\alpha F\eta}{RT}}\right)$ and so $\eta = \frac{RT}{\alpha F} ln \frac{i}{i_0}$. Numerically, an over-potential of 100mV at 25°C is enough to decrease the influence of the second term to 2%. This is an anodic over-potential, so if the electrode is an anode, it is home of oxidation during discharge. If < 0 , $i = -i_0\left(e^{\frac{-(1-\alpha)nF\eta}{RT}}\right)$ and so $\eta = -\frac{RT}{(1-\alpha)nF} ln\left(-\frac{i}{i_0}\right)$. This is a cathodic over-potential, during charge.

To get the amount of energy required for the intercalation and deintercalation process, the following integral has to be computed:

Deintercalation process (during the discharge): $\int_0^I i * \eta(i)di = \int_0^I i * \frac{RT}{\alpha nF} \ln \frac{i}{i_0} di$

Intercalation process (during the charge): $\int_{-I}^0 i * \eta(i)di = \int_{-I}^0 -i * \frac{RT}{(1-\alpha)nF} \ln\left(-\frac{i}{i_0}\right) di = \int_0^I i * \frac{RT}{(1-\alpha)nF} \ln \frac{i}{i_0} di$

The impact of charge or discharge is given by $\frac{1}{\alpha} g_2(I_d) = \frac{1}{1-\alpha} g_2(I_c)$.

Therefore, the two processes require equal energy and therefore equally impact the cell if $\frac{1}{\alpha} = \frac{1}{(1-\alpha)}$, so if $\alpha = \frac{1}{2}$. The energy to intercalate lithium ions during charge and deintercalate during discharge at the cathode is the same [1], therefore $\alpha = \frac{1}{2}$, and therefore the f_2 curve is an odd curve. This latter result is confirmed on NCA related curve in Figure9, where the curves obtained for C/2;1D and 1C;D/2 are parallel, and on Figure 5, the acceptable values of C-rate. For very high C-rate, the behavior of the NCA function is sharply different, and is not explained in this paper.

If the two processes require different energy, $\alpha \neq \frac{1}{2}$. The coefficient twists the curve, and reflects the impact of the growing SEI. From the literature review [3,13], the values obtained for $1 - \alpha$ are 0.69 for a temperature of 25°C, and 0.67 at 45°C. However, Delacourt and al [13] obtained a value of 0.95 at the anode that they judge to be too singular.
Nevertheless, considering $1 - \alpha = \frac{2}{3}$ (which is close to 0.69 and 0.67), it results in $g_2(I_d) = \frac{1}{2} g_2(I_c)$.

So when the rate is “high enough” (then the over-potential is “high enough” as well), we have a relationship between the impact of the charge rates and the discharge ones. The discharge affects the ageing two times less than the charge. This result is confirmed by Bashash and al [12], which shows that battery degradation is slower during discharge than during charge. This paper quantifies it. This seems logical as the ions tend to decrease their potential, and are therefore more stable at the cathode, so when the system is rather discharged. Pushing the ions back to the anode (charging the cell) requires more energy to counterbalance and tends to damage the cell more. The result can be observed on Figure 6 where the discharge impact is twice as big as the charge one for LFP.

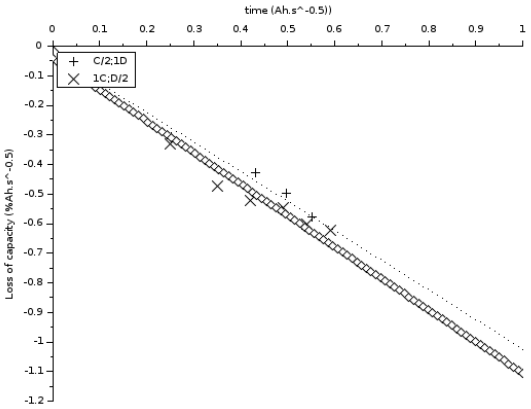

Figure 9 Loss of capacity with respect to CT/√t, for two set of tests : C/2;1D and 1C;D/2. Markers represent experimental values

5.4 Improvements on the tests matrix

It is possible to propose a new test matrix that is more adapted to the needs of the model and to the hardware constraints of the cycling bench and the time constraints. It must be borne in mind that accelerated ageing lasts on average 3 months, and that all cannot be done in parallel, because of the availability of cycling equipment. Better correlation will be obtained by cycling around a SOC point (chosen at 50%) instead of performing 100% DOD cycles (that consists in cycles made of a full discharge and a full charge), because the tests won't heat up.

The "pivot" chosen in the method to obtain the weighting functions has been modified, so that the test does not heat anymore. We obtain the same number of information with less testing. The modified matrix is detailed in Table 3:

Table 3: Tests matrix

	T (°)	SOC (%)	$I_c(A.Ah^{-1})$	$I_d\ (A.Ah^{-1})$
1	T1	80		
2	T2	80		
3	T1	10	1C	1D
4	T1	50	1C	1D
5	T1	80	1C	1D
6	T1	95	1C	1D
7	T1	50	C/2	D/2
8	T2	50	1C	1D
9	T3	50	1C	1D

6 CONCLUSION

This paper compared two Li-ion chemistries in terms of ageing: NCA/graphite and LFP/graphite. The impact of the three ageing parameters has been developed. The similar shapes was explained by similar operating mechanisms, even if the chemistry of the cathode and of the electrolyte were slightly different. The ageing model can be extended to other chemistry, and is coherent with the physical reality of the hidden mechanisms of ageing.

REFERENCES

[1] **Badey, Quentin.** *Étude des mécanismes et modélisation du vieillissement des batteries lithium-ion dans le cadre d'un usage automobile.* s.l. : Thèse de l'Université Paris Sud, 2012.

[2] **I., Bloom et Cole, B.W.** An accelerated calendar and cycle life study – An accelerated calendar and cycle life study of li-ion cells. *Journal of Power Sources.* 2001, pp. A238-A247.

[3] **Aurbach, Doron.** Review of selected electrode–solution interactions which determine the performance of Li and Li ion batteries. *Journal of Power Sources.* 2000, Vol. 89, pp. 206–218.

[4] **Eddahech, Akram.** *Modélisation du vieillissement et détermination de l'état de santé de batteries Li-ion pour application véhicule électrique et hybride.* Bordeaux : s.n., 2013.

[5] **Yoshida, Toshihiro.** Degradation Mechanism and Life Prediction of Lithium-Ion Batteries. *Journl of The Electrochemical Society.* 153, 2006, pp. A576-A582.

[6] **Hemery, Charles-Victor.** *Etude des phénomènes thermiques dans une batterie Li-ion.* Grenoble : s.n., 2013.

[7] **Vetter, J., Novak, P. et Wagner, M.R.** Ageing mechanisms in lithium-ion batteries. *Journal of Power Sources.* 2005, Vol. 147, pp. A269-A281.

[8] **Bashash, Saeid, et al.** Plug-in hybrid electric vehicle charge pattern optimization for energy cost and battery longetivity. *Journal of Power Sources.* 2011, Vol. 196.

[9] *A Model for Predicting Capacity Fade due SEI Formation in a Commercial Graphite/LiFePO4 cell.* **Elkström, Henrik et Lindbergh, Göran.** 162, Stockholm : s.n., 2015.

[10] **Delacourt, C. et Safari, M.** Life Simulation of a Graphite/LiFePO4 Cell under Cycling and Storage. *Journal of the Electrochemical Society.* 2012, Vol. 159, 8.

[11] **Verma, Pallavi, Maire, Pascal et Novak, Pert.** A review of the features and analyses of the solid-electrolyte interphase in Li-ion batteries. *Electrochimica Acta.* 55, 2010, pp. 6332-6341.

[12] **Li, J.** Studies on the cycle life of commercial lithium ion batteries during rapid charge–discharge cycling. *Journal of Power Sources.* 2001, Vol. 102, pp. 294–301.

[13] **Baghdadi, I., et al.** Chemical rate phenomenon approach applied to lithium battery capacity fade estimation. *Microelectronics Reliability.* 2016, Vol. 64, 134-139.

[14] **Chhor, Sarine.** *Etude et modélisation de l'interface graphite/électrolyte dans les batteries Lithium ion.* 2014.